ORIGINAL PAPER

Use of a gradient-generating microfluidic device to rapidly determine a suitable glucose concentration for cell viability test

Chia-Hsien Yeh · Chien-Hsien Chen · Yu-Cheng Lin

Abstract We successfully determined a suitable glucose concentration for endothelial cells (ECs) using a gradient-generating microfluidic chip and a micro-stamper that were fabricated using micro-electro-mechanical systems (MEMS) technology. Our strategy was to generate a stable concentration gradient in the observation area based on a microfluidic network and micro-mixers, which produced a concentration gradient under various flow rates. The areas for cell adhesion were delineated on a glass slide with a micro-stamper using the micro-contact printing (μCP) method. We also discuss which glucose concentration gradients are suitable for cell viability test (i.e., 0–0.2%, 0.05–0.15%, and 0.06–0.17%). After examining various concentration gradients, the suitable glucose concentration for EC's viability test was determined to range from 0.077% (4.2 mM) to 0.147% (8.16 mM). Higher or lower concentrations caused the ECs to atrophy or die. In this study, we describe a gradient-generating microfluidic chip that can be used to produce various drug concentrations for multi-concentration tests.

Keywords Suitable glucose concentrations · Gradient-generating microfluidic chip · Micro-stamper · Micro-contact printing

C.-H. Yeh · C.-H. Chen · Y.-C. Lin (✉)
Department of Engineering Science, National Cheng Kung University, 1 University Road, Tainan 701, Taiwan, ROC
e-mail: yuclin@mail.ncku.edu.tw

Y.-C. Lin
Center for Micro/Nano Technology, National Cheng Kung University, Tainan, Taiwan, ROC

1 Introduction

Concentration gradients of diffusible substances play an important role in many biological processes, such as cell migration, chemotaxis, adaptability, and others. Previous studies have employed chemotaxis chambers (i.e., the Boyden chamber (Somersalo et al. 1990) and under-aga-rose assays) and pipettes to release diffusible substances (Song and Poo 1999) for cell migration. These methods are limited in their abilities to generate concentration gradients and to maintain the gradients for long periods of time (Boyden 1962; Nelson et al. 1975). In a previous study, a microfluidic network device that can generate well-defined stable gradients of solutions was reported (Jeon et al. 2000; Dertinger et al. 2001). Microfluidic devices have since been used to generate gradients in many biological studies. For example, a gradient-generating microfluidic platform was used to optimize the proliferation and differentiation of neural stem cells (NSCs) in culture (Chung et al. 2007). An integrated microfluidic gradient chip was used to analyze lung cancer chemotherapy resistance (Wang et al. 2009). The microfluidic method has several advantages over conventional chemotaxis assays for generating gradients: (1) adjustable gradients can be generated using various network designs, and (2) stable gradients can be maintained for long periods of time. In this study, we developed a gradient-generating microfluidic chip and used it to determine the suitable glucose concentration for endothelial cells (ECs).

Glucose is an important carbohydrate in cell biology. It serves as a source of energy and as a metabolic intermediate. Inappropriate concentrations of glucose are known to have detrimental effects on many cell types. At high concentrations, glucose has multiple deleterious effects on cell metabolism and growth (Yki-Järvinen et al. 1987; Rossetti

et al. 1990; DCCT Research Group 1993). Previous studies have demonstrated that high glucose concentrations lead to a reduction in EC proliferation and a concurrent increase in apoptosis (McGinn et al. 2003; Baumgartner-Parzer et al. 1995). In this study, we designed and employed a micro-fluidic platform to generate a stable glucose concentration in the observation area. Because the ECs are adhesion-type cells, they can easily adhere to glass substrates, and their behavior can clearly be observed by optical microscope. In a recent study, micro-electro-mechanical systems (MEMS) technology was used to fabricate micro-level patterns that allow cells to be cultivated in specific areas on a glass substrate. There are many micro-patterning methods that use MEMS technology for the analysis of organisms, including photolithography (Park and Shuler 2003; Folch and Toner 2000; Wyart et al. 2002), micro-contacting printing (μCP) (Katanosaka et al. 2008; Das et al. 2007), micro-molding in capillaries (MIMIC) (Kim et al. 2001; Li et al. 2007), laminar flow patterning (Takayama et al. 1999, 2001a, b), and stencil patterning (Folch et al. 2000). In 1998, a PDMS impression device was used to imprint poly-lysine onto a glass substrate using the μCP method to position cells (Branch et al. 1998). Chang et al. (2003) also applied the μCP method to position nerve cells onto electrodes. This method was chosen because the μCP method is more convenient to use than other methods to define the adhesion position and area for cells. Also, the micro-stamper is composed of PDMS, which is elastic and has high biocompatibility. In our study, the μCP method was used to determine specific cultivation patterns for ECs by imprinting the micro-stamper coated with the chemical materials onto the glass substrate. The micro-stamper was therefore used to uniformly imprint BSA solution onto the observation area to define the area of cell adhesion.

In our study, we determined a suitable glucose concentration for cell viability test using a gradient-generating microfluidic chip and a micro-stamper. The gradient-generating microfluidic chip and micro-stamper were fabricated using MEMS technology. The linear concentration gradient was controlled by adjusting various flow rates. The micro-stamper was used to define the cell adhesive/non-adhesive areas using the μCP method. By examining various glucose concentration gradients (0–0.2%, 0.05–0.15%, and 0.06–0.17%), the glucose concentration that was most suitable for ECs was determined to range from 0.077 to 0.147% under a flow rate of 20 μl/min. The microfluidic platform that we developed was advantageous for several reasons: (1) cell adaptation was clearly observed in the stable concentration gradient produced on the microfluidic chip, and (2) it was convenient to observe changes in cell behavior using the μCP method with the gradient-generating microfluidic chip. In the future, the microfluidic platform that we developed may be used to generate concentration gradients of various drugs, which can be studied using a variety of cell types.

2 Materials and methods

2.1 Chemical reagents

Fetal bovine serum (FBS), trypsin–EDTA, phosphate-buffered saline (PBS), Dulbecco's Modified Eagle's Medium (DMEM), penicillin–streptomycin (PS), L-glutamine, sodium pyruvate were all purchased from Gibco, Invitrogen Corporation. Sodium bicarbonate, bovine serum albumin (BSA), trypan blue, and glucose were obtained from Sigma-Aldrich Corporation. The glucose solution contained a mixture of 1 g glucose powder and 1 l D.I. water. Five percent BSA contained a mixture of 0.5 g BSA and 10 ml PBS, and it was stored at 4°C.

2.2 Cell culture

MS-1 cells are murine ECs, kindly provided by Dr. Jiang MJ at National Cheng Kung University. Because these ECs are of the adhesion-type, cell morphology and cell growth could clearly be observed using an optical microscope. The cells were cultured in medium that included 13.5 g DMEM, 1.5 g sodium bicarbonate, 10% FBS, 1% PS, 1% sodium pyruvate, 1% L-glutamine, and l l D.I. water. The cells were sub-cultured every 2–3 days.

2.3 Design and fabrication of a gradient-generating microfluidic chip and micro-stamper

The gradient-generating microfluidic chip and micro-stamper were designed using AutoCAD® 2008. This gradient-generating microfluidic chip included a microfluidic network and micro-mixers. The concentration distribution ranged from layer I to layer IX in the observation area, which was connected to the area of cell adhesion on the glass slide, as shown in Fig. 1a. The width of the micro-mixer layout was 100 μm in the microchannel, as shown in Fig. 1b. The area of cell adhesion was 300 μm wide and 1 mm long, and the gap between the two strips of cell adhesion was 200 μm, as shown in Fig. 1c. The gradient-generating microfluidic chip and micro-stamper had a depth of 100 μm.

Fabrication of the gradient-generating microfluidic chip and the micro-stamper involved production of the SU-8 pattern followed by the production of the PDMS chip. First, the SU-8 microstructure pattern was fabricated in the silicon wafer using MEMS technology, including spin coating, exposure, and developing. After completion of the SU-8 pattern, replica mold technology was used to fabricate the PDMS chip. PDMS liquid was poured into the

Fig. 1 **a** The various concentration gradients generated in the observation area using the microfluidic network and micro-mixers. **b** The design of the micro-mixers, the unit: mm. **c** The observation area: the cell adhesion area produced using a micro-stamper
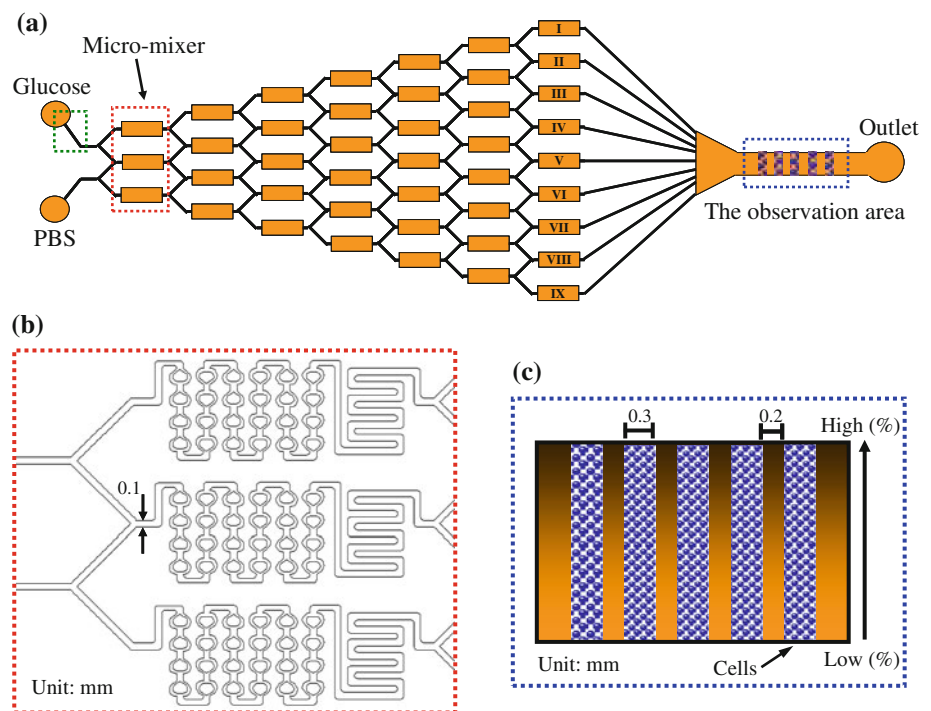
SU-8 pattern, and the PDMS chip was peeled away from the SU-8 pattern after 40 min of incubation in a 70°C oven.

2.4 The micro-contact printing method

A micro-stamper was used to define the areas of cell adhesion. Because cells do not adhere to the surface of the BSA solution, the pattern of BSA solution on the glass slide determined the areas of cell adhesion. The BSA pattern on the glass slide was defined using the μCP method. First, the surface of the micro-stamper was used to change the functional groups from CH_3 groups to OH groups using an oxygen plasma machine (In-line plasma cleaner, NEWST-2002IL). The parameters for oxygen plasma treatment were 75 mTorr, 150 W of RF power, and a treatment time of 10 min. After a surface change was induced using the oxygen plasma treatment, the micro-stamper was soaked in 5% BSA solution for 2 h. After soaking, the excess BSA solution in the micro-stamper was removed using nitrogen gas. Then the micro-stamper was pressed slightly onto a glass slide for 2 min. The micro-stamper was then removed, and the glass slide that contained the BSA pattern was dried for 12 h and sterilized using ultraviolet light. ECs did not grow on areas of the glass slide that contained BSA, even after 12 h of cultivation.

2.5 The experimental process

After the BSA pattern (in Sect. 2.4) was defined on the glass slide using the μCP method, the surface of the gradient-generating microfluidic chip was modified using an oxygen plasma treatment (75 mTorr, 150 W of RF power, and 30 s), and the microfluidic chip was then bonded to the glass slide. Because the length of the PDMS micro-stamper was 1 cm, and the length of the observation area was 1 mm, we aligned the observation area of the PDMS layer to the BSA-patterned glass carefully to define the cell adhesion area. After being sterilized for 12 h, the ECs were injected into the microfluidic chip. The process is shown in Fig. 2. After the ECs were cultivated for 12 h, two different concentrations of glucose solution were injected into the gradient-generating microfluidic chip using a syringe pump (KDS230, USA) to generate a concentration gradient in the observation area (i.e., the area in which the ECs grew along the cell adhesion area). Because the concentration gradient and the cell adhesion ability were influenced by the flow rate, various flow rates (10, 20, 30, 40, and 50 μl/min) were tested. Moreover, to find the suitable glucose concentration for EC's viability test, different concentration intervals (0–0.2%, 0.05–0.15%, and 0.06–0.17%) were tested in turn.

2.6 Microscope measurement

The experimental images were observed using an optical microscope (BX60, Olympus, Japan) and a digital camera (DP70, Olympus, Japan). The concentration gradients of the trypan blue solution were analyzed using Photoshop® and ImageJ software.

Fig. 2 The experimental processes for producing BSA patterns and bonding between the PDMS microfluidic chip and the glass slide
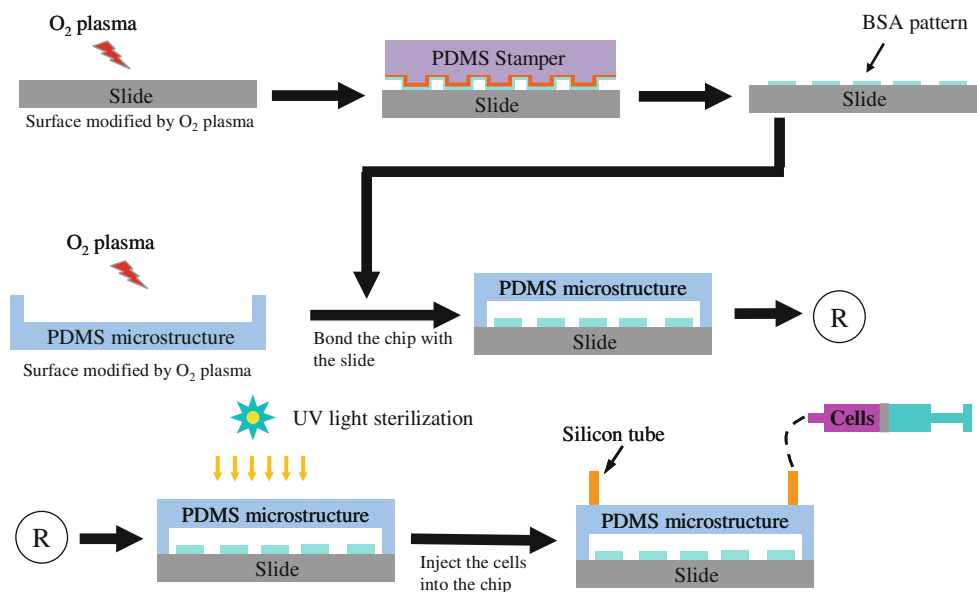
3 Results and discussion

### 3.1 SEM of the SU-8 pattern

After using MEMS technology to fabricate the SU-8 pattern, the microstructure was measured using a scanning electron microscope (SEM). The surface of the SU-8 pattern was very smooth, and the microstructure matched the mask design, as shown in Fig. 3a and b. Figure 3a shows the solution injection region, and Fig. 3b shows the micromixer region. The height of the SU-8 pattern was 100 μm. The gradient-generating microfluidic chip and microstamper were fabricated by replicating the SU-8 pattern.

3.2 Concentration gradient results

The gradient-generating microfluidic chip used a microfluidic network and micro-mixers to generate nine different layers of concentration flow in the observation area. For concentration analysis, the concentration of each layer was used to calculate the grayscale using ImageJ software. To measure the PBS concentration gradient, we treated the 1× PBS solution and the pure trypan blue solution as PBS concentrations of 100 and 0%, respectively, and injected them into the microfluidic chip. The different PBS concentration distributions were observed after they were uniformly mixed. Under different flow rates (10, 20, 30, 40, and 50 μl/min), different concentration gradients were generated in the observation area; the grayscale of each concentration gradient is shown in Fig. 4a–d. In the grayscale analysis, the non-linear concentration gradient occurred at a flow rate of 10 μl/min. When the flow rate was increased from 20 to 50 μl/min, the grayscale was linearly uniform at each flow rate. To prevent the flow rate from affecting experimental accuracy, a flow rate of 20 μl/min was used in the experiment. Finally, the average grayscale of each concentration layer was obtained using Photoshop® software, and the concentration percent of each layer was calculated using the interpolation method, as shown in Fig. 4e. By controlling the concentrations of two injected

Fig. 3 SEM images of the SU-8 pattern **a** sample inlet region and **b** micro-mixer region located in the *green* and *red dotted square* of Fig. 1a, respectively. The SU-8 pattern is 100 μm deep
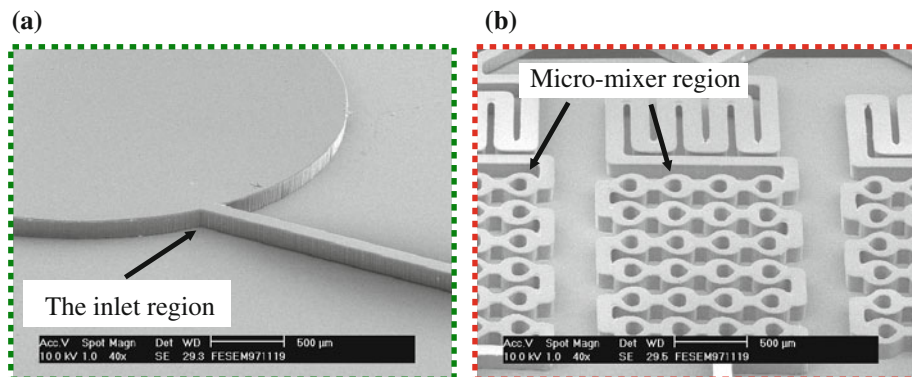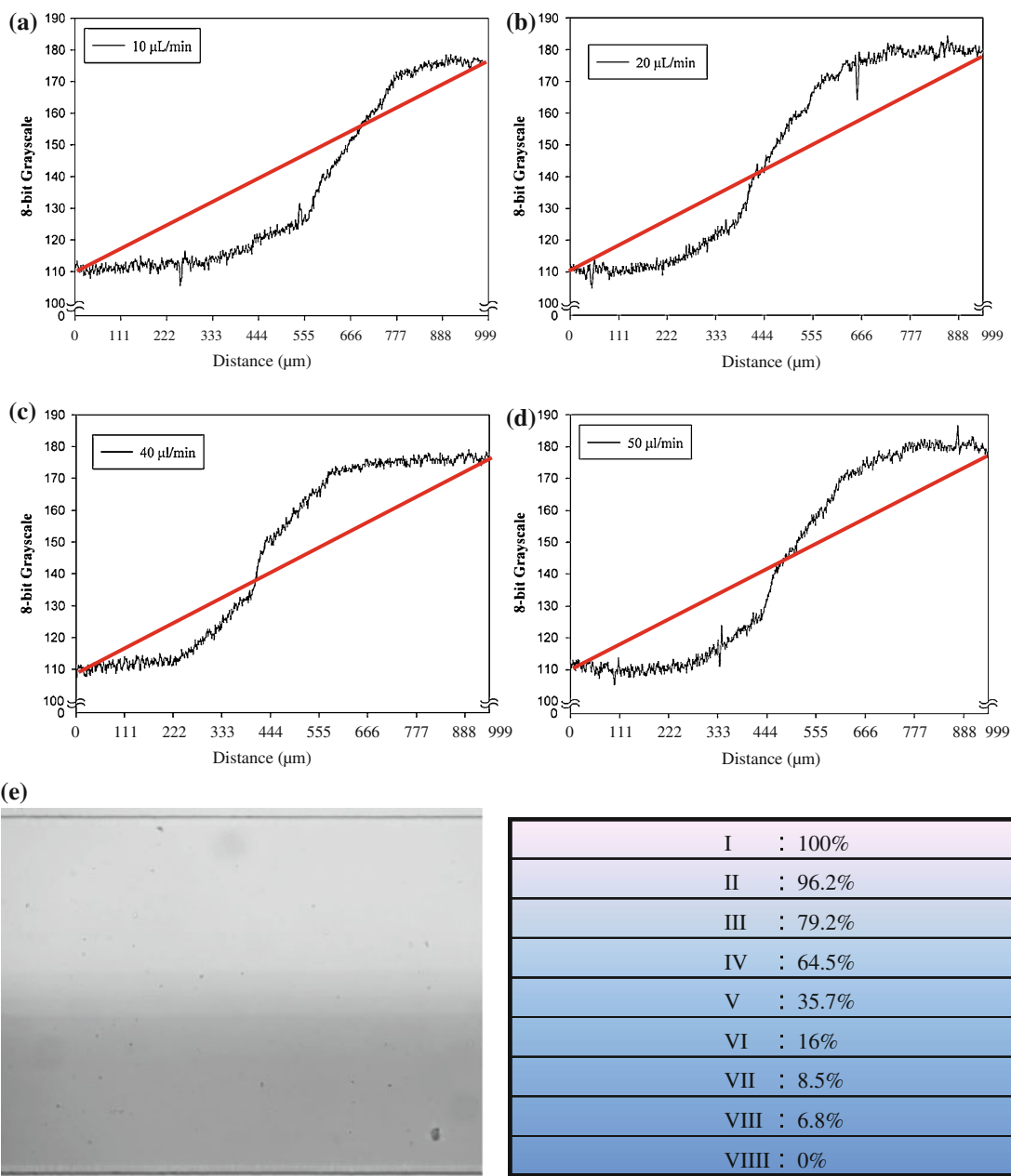
Fig. 4 Grayscale analysis of different flow rates in the observation area. The trypan blue solution and the PBS buffer solution were injected into the microfluidic chip, and the grayscale of each flow rate were analyzed using ImageJ software. The results obtained under a flow rate of **a** 10 μl/min, **b** 20 μl/min, **c** 40 μl/min, and **d** 50 μl/min. **e** The percent concentration of each layer under a flow rate of 20 μl/min was calculated using the interpolation method

glucose solutions, the glucose concentration of each layer could be calculated. Because the trypan blue and glucose were both dissolved in water, the glucose solutions (0.05, 0.06, 0.15, 0.17, and 0.2%) and the trypan blue solution (0.4%) had similar viscosities, densities, and spreading coefficients. The glucose concentration gradient was therefore the same as the observed grayscale of the trypan blue concentration gradient.

3.3 The suitable glucose concentration for ECs

After the ECs were cultivated in the observation area for 12 h, two different glucose solutions were injected into the gradient-generating microfluidic chip at a flow rate of 20 μl/min. Three concentration gradient ranges were used in this experiment, i.e., 0–0.2%, 0.05–0.15%, and 0.06–0.17%; the concentration of each layer is shown in

Table 1 The concentration distribution of different concentration gradients in each layer

| Layer	Glucose concentration distribution (%)		
I	0.2	0.15	0.17
II	0.192	0.146	0.165
III	0.158	0.129	0.147
IV	0.12	0.114	0.131
V	0.071	0.086	0.099
VI	0.032	0.066	0.077
VII	0.017	0.058	0.069
VIII	0.013	0.056	0.067
IX	0	0.05	0.06

Table 1. According to reference (Kim et al. 2006), the shear stress of the rectangular shape channel can be described using the parallel plate model. The fluid shear formula on the cells would equal the shear stress (Γ) at the wall between parallel plates under parabolic flow,

$$\Gamma = \frac{6\mu Q}{h^2 w} \tag{1}$$

where Q is the volumetric flow rate, h is the height of the channel, μ is the fluid viscosity, and w is the width of the channel. In the observation area of this chip, the shear stress was 1.78 dyne/cm^2 under a flow rate 20 μl/min. In previous studies (Dewey et al. 1981; Wechezak et al. 1985), the shear stress effect on the ECs was in excess of 7 dyne/cm^2, so in this study, the shear stress effect on ECs was not considered. Moreover, in order to avoid the edge effect for ECs in concentration gradient distribution, the glucose concentrations of layer I and layer IX were ignored.

In the concentration gradient that ranged from 0 to 0.2%, the ECs in the non-adhesion area were removed by
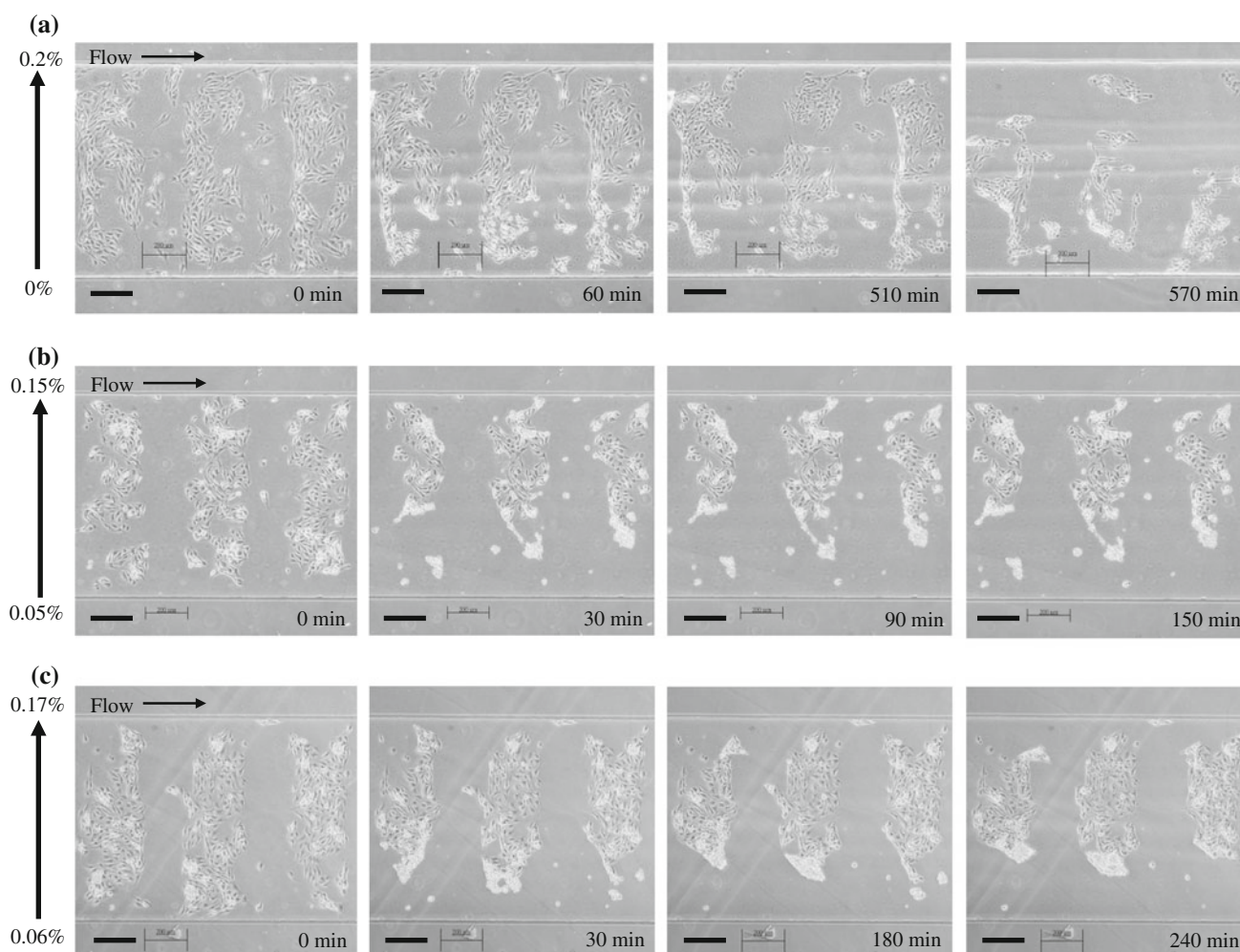

Fig. 5 Real-time observation of the ECs under different concentration gradients. The varying concentration gradients of glucose solution were generated in the observation area, and the ECs gradually appeared to atrophy as the observation time increased. **a** The concentration gradient ranged from 0 to 0.2%, **b** the concentration gradient ranged from 0.05 to 0.15%, and **c** the concentration gradient ranged from 0.06 to 0.17% (scale bar: 200 μm)

the glucose flow when the glucose solution was injected into the microfluidic chip. The ECs in glucose concentrations ranging from 0 to 0.071% exhibited atrophy after 60 min. After 510 min, the ECs exposed to the glucose concentration gradient of 0.158 to 0.2% began to come off the cell adhesion area. Finally, the observation area containing a glucose concentration distribution from 0.12 to 0.158% had not obviously changed after 570 min, as shown in Fig. 5a. According to these results, this study shows that we can successfully generate a stable concentration gradient that can be used to determine a suitable concentration distribution for cells.

In Fig. 5a, the ECs became atrophic in 60 min in glucose concentrations ranging from 0 to 0.071%. The ECs were then removed from the cell adhesion area from 0.158 to 0.2% after 510 min. To determine the glucose concentration distribution that was suitable for ECs, the concentration gradient was adjusted from 0–0.2% to 0.05–0.15%. It is obvious that the ECs appeared to exhibit atrophic conditions when exposed to glucose concentrations of 0.05 to 0.086% and 0.146 to 0.15% after 30 min. When the observation time was increased, there was no obvious change in the observation area, as shown in Fig. 5b. For example, the number of cells in layer II was 20 from 0 to 120 min, and the number of cells in layer V was about 22 from 30 to 120 min. These results show that it is suitable for ECs to grow in glucose concentrations ranging from 0.086 to 0.146%. To check the glucose concentration at the boundaries of the gradient, the glucose concentration gradient of 0.06 to 0.17% was used. The ECs exhibited atrophic conditions at concentrations ranging from 0.06 to 0.077% and from 0.147 to 0.17% after 180 min. When the observation time was increased, there was no obvious change in the observation area, as shown in Fig. 5c. For example, the cell number in layer III was 21 from 0 to 240 min, and the cell number in layer V was about 28 from 120 to 240 min. According to these concentration gradient tests, the suitable range of glucose concentration for EC's viability test is from 0.077 to 0.147%. Under the 0.06, 0.1, and 0.17% of glucose concentration, the non-flowing condition for ECs was observed at 0, 2, 4, and 6 h. We can find the ECs were normally cultivated from 0 to 6 h under the 0.1% of glucose concentration. But, we can find the ECs were atrophic and death from 4 to 6 h under the 0.06 and 0.17% of glucose concentration (data not shown). So the unsuitable concentration for ECs under the non-flowing condition caused the ECs death.

Based on the results from experiments that examined concentration gradients ranging from 0.05 to 0.15% and 0.06 to 0.17%, the cell number for each concentration layer was counted, as shown in Fig. 6. In the 0.05–0.15% concentration gradient, the cell number obviously decreased from layer VI (0.066%) to IX (0.05%) when the
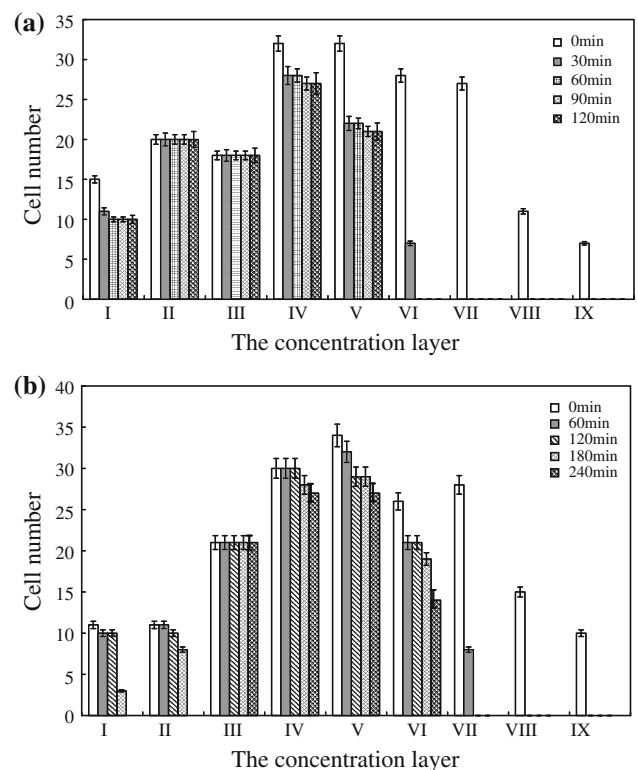
Fig. 6 The relationship between the number of cells and the glucose concentration in each layer at different observation times. **a** The concentration gradient ranged from 0.15 to 0.05%, and **b** the concentration gradient ranged from 0.17 to 0.06%

experimental time was increased. The suitable concentration for ECs ranged from 0.146% (layer II) to 0.086% (layer V), as shown in Fig. 6a. Finally, in the boundary concentration gradient test in the area ranging from 0.06 to 0.17%, the cell numbers were not obviously different between layers III (0.147%) and VI (0.077%), and the suitable concentration distribution of glucose solution for EC's viability test ranged from 0.077 to 0.147%, as shown in Fig. 6b.

4 Conclusions

A gradient-generating microfluidic chip and micro-stamper have successfully been used to determine a suitable glucose concentration for EC's viability test. By generating concentration gradients in the observation area and defining the areas of cell adhesion on glass slides by employing a micro-stamper using the μCP method, a suitable glucose concentration for EC's viability test was determine to range from 0.077% (4.2 mM) to 0.147% (8.16 mM) under a flow rate of 20 μl/min. The normal glucose concentration in the human body for ECs is 5.5 mM (Millioni et al. 2010). The device described in this study can be used in future investigations to produce different ranges of drug

concentrations to rapidly determine suitable concentration distributions for specific cells.

References

Baumgartner-Parzer SM, Wagner L, Pettermann M, Grillari J, Gessl A, Waldhausl W (1995) High-glucose-triggered apoptosis in cultured endothelial cells. Am Diabetes Assoc 44:1323–1327

Boyden SV (1962) Rapid quantitation of neutrophil chemotaxis: use of a polyvinylpyrrolidone-free polycarbonate membrane in a multiwell assembly. J Immunol Methods 115:453–466

Branch DW, Corey JM, Weyhenmeyer JA, Brewer GJ, Wheeler BC (1998) Microstamp patterns of biomolecules for high-resolution neuronal networks. Med Biol Eng Comput 36:135–141

Chang JC, Brewer GJ, Wheeler BC (2003) A modified microstamping technique enhances polylysine transfer and neuronal cell patterning. Biomaterials 24:2863–2870

Chung BG, Park JW, Hu JS, Huang C, Monuki ES, Jeon NL (2007) A hybrid microfluidic-vacuum device for direct interfacing with conventional cell culture methods. BMC Biotechnol 7:60–67

Das T, Mallick SK, Paul D, Bhutia SK, Bhattacharyya TK, Maiti TK (2007) Microcontact printing of concanavalin a and its effect on mammalian cell morphology. J Colloid Interface Sci 314:71–79

DCCT Research Group (1993) The effect of intensive treatment of diabetes on the development and progression of long-term complications in insulin-dependent diabetes mellitus. N Engl J Med 329:977–986

Dertinger KWS, Chiu DT, Jeon NL, Whitesides GM (2001) Generation of gradients having complex shapes using microfluidic networks. Anal Chem 73:1240–1246

Dewey CF, Bussolari SR, Gimbrone MA, Davies PF (1981) The dynamic response of vascular endothelial cells to fluid shear stress. J Biomech Eng 103:177–185

Folch A, Toner M (2000) Microengineering of cellular interactions. Annu Rev Biomed Eng 2:227–256

Folch A, Jo BH, Hurtado O, Beebe DJ, Toner M (2000) Microfabricated elastomeric stencils for micropatterning cell cultures. J Biomed Mater Res 52:346–353

Jeon NL, Dertinger SKW, Chiu DT, Choi IS, Stroock AD, Whitesides GM (2000) Generation of solution and surface gradients using microfluidic systems. Langmuir 16:8311–8316

Katanosaka Y, Bao JH, Komatsu T, Suemori T, Yamada A, Mohri S, Naruse K (2008) Analysis of cyclic-stretching responses using cell-adhesion-patterned cell. J Biotechnol 133:82–89

Kim YD, Park CB, Clark DS (2001) Stable sol-gel microstructured and microfluidic networks for protein patterning. Biotechnol Bioeng 73:331–337

Kim L, Vahey MD, Lee HY, Voldman J (2006) Microfluidic arrays for logarithmically perfused embryonic stem cell culture. Lab Chip 6:394–406

Li Y, Yuan B, Ji H, Han D, Chen S, Tian F, Jiang X (2007) A method for patterning multiple types of cells by using electrochemical desorption of self-assembled monolayers within microfluidic channels. Angew Chem Int Ed 46:1094–1096

McGinn S, Poronnik P, King M, Gallery EDM, Pollock CA (2003) High glucose and endothelial cell growth: novel effects independent of autocrine TGF-beta 1 and hyperosmolarity. Am J Physiol Cell Physiol 284:1374–1386

Millioni R, Puricelli L, Iori E, Arrigoni G, Tessari P (2010) The effects of rosiglitazone and high glucose on protein expression in endothelial cells. J Proteome Res 9:578–584

Nelson RD, Quie PG, Simmons RL (1975) Chemotaxis under agarose: a new and simple method for measuring chemotaxis and spontaneous migration of human polymorphonuclear leukocytes and monocytes. J Immunol 115:1650–1656

Park TH, Shuler ML (2003) Integration of cell culture and microfabrication technology. Biotechnol Prog 19:243–253

Rossetti L, Giaccari A, DeFronzo RA (1990) Glucose toxicity. Am Diabetes Assoc 13:610–630

Somersalo K, Salob OP, Bjorkstenb F, Mustakallioc KK (1990) A simplified Boyden chamber assay for neutrophil chemotaxis based on quantitation of myeloperoxidase. Anal Biochem 185:238–242

Song H, Poo MM (1999) Signal transduction underlying growth cone guidance by diffusible factors. Curr Opin Neurobiol 9:355–363

Takayama S, McDonald JC, Ostuni E, Liang MN, Kenis PJA, Ismagilov RF, Whitesides GM (1999) Patterning cells and their environments using multiple laminar fluid flows in capillary networks. Proc Natl Acad Sci USA 96:5545–5548

Takayama S, Ostuni E, Qian XP, McDonald JC, Jiang XY, LeDuc P, Wu MH, Ingber DE, Whitesides GM (2001a) Topographical micropatterning of poly(dimethylsiloxane) using laminar flows of liquids in capillaries. Adv Mater 13:570–574

Takayama S, Ostuni E, LeDuc P, Naruse K, Ingber DE, Whitesides GM (2001b) Laminar flows-subcellular positioning of small molecules. Nature 411:1016

Wang S, Yue F, Zhang L, Wang J, Wang Y, Jiang L, Lin B, Wang Q (2009) Simultaneous quantification of active components in the herbs and products of Si-Wu-Tang by high performance liquid chromatography-mass spectrometry. J Pharm Biomed Anal 49:806–810

Wechezak AR, Viggers RF, Sauvage LR (1985) Fibronectin and F-actin redistribution in cultured endothelial cells exposed to shear stress. Lab Invest 53:639–647

Wyart C, Ybert C, Bourdieu L, Herr C, Prinz C, Chatenay D (2002) Constrained synaptic connectivity in functional mammalian neuronal networks grown on patterned surfaces. J Neurosci Methods 117:123–131

Yki-Järvinen H, Helve E, Koivisto VA (1987) Hyperglycemia decreases glucose uptake in type I diabetes. Am Diabetes Assoc 36:892–896